Journal of Mathematical Biology (2018) 77:1563–1588
https://doi.org/10.1007/s00285-018-1263-5

Mathematical Biology

Host contact structure is important for the recurrence of Influenza A

J. M. Jaramillo[1] · Junling Ma[1] · P. van den Driessche[1] · Sanling Yuan[2]

Received: 12 April 2017 / Revised: 5 June 2018 / Published online: 4 July 2018
© Springer-Verlag GmbH Germany, part of Springer Nature 2018

Abstract
An important characteristic of influenza A is its ability to escape host immunity through antigenic drift. A novel influenza A strain that causes a pandemic confers full immunity to infected individuals. Yet when the pandemic strain drifts, these individuals will have decreased immunity to drifted strains in the following seasonal epidemics. We compute the required decrease in immunity so that a recurrence is possible. Models for influenza A must make assumptions on the contact structure on which the disease spreads. By considering local stability of the disease free equilibrium via computation of the reproduction number, we show that the classical random mixing assumption predicts an unrealistically large decrease of immunity before a recurrence is possible. We improve over the classical random mixing assumption by incorporating a contact network structure. A complication of contact networks is correlations induced by the initial pandemic. We provide a novel analytic derivation of such correlations and show that contact networks may require a dramatically smaller loss of immunity before recurrence. Hence, the key new insight in our paper is that on contact networks the establishment of a new strain is possible for much higher immunity levels of previously infected individuals than predicted by the commonly used random mixing assumption. This suggests that stable contacts like classmates, coworkers and family members are a crucial path for the spread of influenza in human populations.

Keywords Influenza · Antigenic drift · Reproduction number · Correlations · Contact network

Mathematics Subject Classification 92D30

✉ Junling Ma
junlingm@uvic.ca

[1] Department of Mathematics and Statistics, University of Victoria, Victoria, BC, Canada

[2] College of Science, Shanghai University for Science and Technology, Shanghai, China

1 Introduction

Seasonal influenza is an acute viral infection that is transmitted easily from person to person and circulates worldwide. It is commonly referred to as 'the flu'. There are three main types (A, B, C) of seasonal influenza viruses, however, types A and B are the causes of most outbreaks and epidemics. Influenza A viruses are further classified by subtypes according to the combination of two surface proteins, haemagglutinin (HA) and neuraminidase (NA). The subtypes of influenza A virus currently in circulation are A(H3N2) and A(H1N1)pdm09 (WHO 2016). Influenza spreads easily from person to person via infectious droplets dispersed by sneezing, coughing or talking (Cox and Subbarao 2000). The social and economic burden of seasonal influenza is significant; an estimated 5–15% are infected every year resulting in suffering and a high loss of economic productivity due to worker absenteeism (WHO 2016).

In this paper, we focus on influenza A. In general, a major challenge with influenza A is its fast scaled evolution. Significant evolution is thought to occur on the timescale of 1 year (Earn et al. 2002). This evolution allows the evolving strain(s) to modify antigenic surface HA and NA proteins (Both et al. 1983); allowing the virus to re-infect a host who had been previously infected and had recovered with full immunity to the infecting strain (Carrat and Flahault 2007; Perez et al. 2010). The processes that result in genetic modification to surface proteins are referred to as antigenic drift and antigenic shift. Antigenic shift is a sudden, dramatic variation of antigenic genes often caused by a re-assortment among distinct strains, and effectively results in a novel strain unrecognizable to host immunity (Earn et al. 2002). These shifts are believed to be random, and may give rise to large scale pandemics (Carrat and Flahault 2007). Such examples include the notorious 1918 Spanish flu, and more recently the 2009 H1N1 pandemic (WHO 2016). While antigenic shift results in a dramatic antigenic variation, antigenic drift is a more subtle mechanism acting by way of frequent, point mutations at the antigenic sites of the virus; allowing the strain to drift away from recognition by the host's immune system (Carrat and Flahault 2007). These two mechanisms are responsible for an important pattern for influenza A: first, a novel and highly virulent influenza strain emerges as a result of antigenic shift, causes a pandemic, and through antigenic drift may return to cause subsequent epidemics as a seasonal strain. In fact, all circulating influenza viruses are drift products of previous pandemic influenza strains (Carrat and Flahault 2007). For example, in April 2009, a novel influenza A(H1N1) virus emerged and caused the first pandemic of the twenty-first century. Referred to as A(H1N1)pdm09, it remains as one of the currently circulating influenza A strains (WHO 2016).

Immediately after a pandemic, there is a reduced pool of susceptible individuals and thus selective pressure drives the antigenic drift process so that the virus can re-invade the population (Bush et al. 1999). This leads to the important question: How much antigenic drift is necessary to cause a first recurrence of the pandemic strain? To address this question we formulate a mathematical framework to model the pandemic and invasiveness of a drifted strain in subsequent seasons.

2 Framework

Many mathematical models for the ecological and epidemic dynamics of influenza have been formulated and analyzed. Some models have built on the fundamental SIR compartmental model of Kermack and McKendrick (1927) to include, for example, several drifted strains. For a few examples of influenza models; see Andreasen et al. (1997); Andreasen (2003), Asaduzzaman et al. (2015), Casagrandi et al. (2006), Pease (1987) and for a review see Earn et al. (2002). A standard tool that we employ is the basic reproduction number ($\mathscr{R}_0$). It is a model-dependent value that determines the vulnerability of a population to an epidemic. Generally speaking, in infectious disease models, if $\mathscr{R}_0 > 1$, an infection-free population is vulnerable to an epidemic. For $\mathscr{R}_0 < 1$, the introduction of a few infected individuals is not expected to cause an epidemic.

Most existing models for influenza make the random mixing assumption. Roughly speaking, this means that any individual interacts randomly with other individuals. On the other end of this spectrum, individuals interact within a fixed set of contacts, and that the number of these contacts varies from individual to individual. This is effectively a social contact network, where individuals are represented by nodes, and adjacent nodes (two nodes with an edge connecting them) are seen as contacts. It is known that network models differ in predictions from classical random mixing models; see, for example, Chatterjee and Durrett (2009), Eames and Keeling (2002), Lindquist et al. (2011), Miller (2011), Pastor-Satorras and Vespignani (2001). In addition, network structure changes the fitness of invading strains (Leventhal et al. 2015). Thus, here we compare results from fixed network models to those of random mixing models. Biologically, our models separate the time scale for the evolution of the pandemic strain and that of the pandemic. This is justified since at the introduction of a new novel influenza A strain to which there is little to no population immunity, evolution via antigenic selection is small; resulting in lower levels of antigenic drift relative to the pandemic dynamics. Furthermore the low levels of antigenic drift result in antigenic homogeneity for circulating strain of influenza A. This was in in fact the case for the 2009 H1N1 outbreak, and we infer this to be true for pandemic strains in general (Garten et al. 2009). Note that antigenic homogeneity cannot be generally applied to seasonal strains because antigenic diversity is present and important within a single season (Besselaar et al. 2004; Kang et al. 2010; Strelkowa and Lässig 2012). Following the end of the pandemic wave (also referred to as the "first wave" in this paper) we look at whether or not challenges by drifted strains are capable of causing an outbreak in a population affected by the first wave. It should also be noted that although many drifted strains could be circulating outside of the population in question (Russell et al. 2008), an imported strain is successful in invading if only if the second wave system has a reproduction number greater than one ($\mathscr{R}^{(2)} > 1$).

Mathematically, this translates into a two-step system where a first wave or pandemic is modelled using a standard SIR model, and the final state is fed into a modified (SAIR) model in which recovered individuals in the first wave become partially susceptible (A) to a drifted strain in the second wave. We refer to the (SAIR) model as the second wave system. This approach of modelling the pandemic and the season after the pandemic may be seen as a truncation of Andreasen's model (Andreasen

2003). However, here we add a layer of complexity by studying the effects of differing population structure assumptions. As the fundamental goal is to understand effects of host population structure, we do not include seasonality and demographic effects.

The general organization of this paper is as follows. In Sects. 3 and 4 we demonstrate the use of the two step process for the pandemic and first return of the strain for random mixing models including homogeneous and heterogeneous random mixing. For random mixing models, we find in general that $\mathscr{R}^{(2)} > 1$ (i.e., a second wave occurs) only after large amounts of antigenic drift. This is contrary to reported observations of subsequent waves that were caused by mutants of the H1N1 pandemic strains that were antigenically indistinguishable from the (H1N1)pdm09 pandemic strain (Barr et al. 2010; El Rhaffouli et al. 2014; Hoschler et al. 2012; Russo et al. 2014). Therefore in Sect. 5, we repeat the process under the random contact network framework and find that re-invasion is possible at much lower levels of antigenic drift.

3 Fully homogeneous SIR model

3.1 First wave dynamics

With no heterogeneity, the first wave is described by the classic Kermack–McKendrick SIR model (Kermack and McKendrick 1927) that assumes random mixing. Taking S, I, R as the fraction of individuals who are susceptible, infectious, and recovered respectively, the dynamics are given by the equations

$$\begin{aligned} S' &= -\tilde{\beta} SI \\ I' &= \tilde{\beta} SI - \gamma I \\ R' &= \gamma I \end{aligned}$$

Here $\tilde{\beta}$ is the transmission rate and γ is the recovery rate. Note that by ignoring demographic effects, $S + I + R = 1$. The initial conditions are given by $S(0) \approx 1$, $I(0) \approx 0$, $R(0) = 0$.

The first wave basic reproduction number $\mathscr{R}_0^{(1)}$ is given by the ratio $\frac{\tilde{\beta}}{\gamma}$; see for example, Brauer et al. (2008). If $\mathscr{R}_0^{(1)} > 1$, then an epidemic occurs and the final state is given by the solution to the relation

$$S_\infty = e^{-\mathscr{R}_0^{(1)}(1-S_\infty)} \tag{1}$$

along with limiting values $I_\infty = 0$, $R_\infty = 1 - S_\infty$ (see, for example, Brauer et al. (2008); Kermack and McKendrick (1927)).

3.2 Second wave dynamics

Throughout this paper we assume that antigenic drift causes an increase in susceptibility among the recovered individuals, but does not change infectivity or the infectious

period. Thus, for the remainder of this paper, we refer to antigenic drift, an increase in susceptibility and drop in immunity interchangeably. For the second wave caused by a drifted strain, individuals recovered from the first wave become partially susceptible to this new strain with susceptibility $\sigma \in [0, 1]$. The fraction of the partially susceptible individuals is denoted by A. Of course, the values $\sigma = 0$ and $\sigma = 1$ correspond to no and full susceptibility, respectively, and the initial conditions are $A(0) \approx 1 - S_\infty$, $S(0) \approx S_\infty$, $I(0) \approx 0$, $R(0) = 0$. The SAIR dynamics are given by the equations

$$\begin{aligned} S' &= -\tilde{\beta} S I \\ A' &= -\sigma \tilde{\beta} A I \\ I' &= (\tilde{\beta} S + \sigma \tilde{\beta} A) I - \gamma I \\ R' &= \gamma I \end{aligned}$$

The reproduction number for the second wave is given by $\mathscr{R}^{(2)} = \frac{\tilde{\beta}}{\gamma}(S(0) + \sigma A(0))$, which may be reformulated using $\mathscr{R}_0^{(1)} = \frac{\tilde{\beta}}{\gamma}$ as

$$\mathscr{R}^{(2)} = \mathscr{R}_0^{(1)} S_\infty + \sigma \mathscr{R}_0^{(1)} (1 - S_\infty) \tag{2}$$

where S_∞ is given by (1). This expression for $\mathscr{R}^{(2)}$ depends linearly on σ. For example, if $\mathscr{R}_0^{(1)} = 2$, then $\mathscr{R}^{(2)} > 1$ for $\sigma > 0.373$ (i.e., an outbreak). This gives the susceptibility threshold, $\sigma_T = 0.373$. Thus, in order for a recurrence to be possible, the virus must undergo significant antigenic drift before it may cause another epidemic. This is larger than the observed value of $\sigma_T \approx 0.25$ for influenza A(H3N2) (Kucharski et al. 2015); see also Klein et al. (2014). This suggests that our model needs to be refined to capture this effect.

4 Multi-group SIR model

If the underlying population is not homogeneous in the number of contacts, then incorporating heterogeneities has been found to be important (Hethcote and Van Ark 1987; Pastor-Satorras and Vespignani 2001). A first approach in this direction is to incorporate heterogeneities by classifying individuals by the average number of individuals they randomly contact on a daily basis, which is effectively a multi-group model; see, for example, Hethcote and Van Ark (1987). Let S_k, I_k, R_k denote the fraction of susceptible, infectious, recovered individuals with k contacts per day. We assume that an individual has contacts with individuals at a rate proportional to their number of contacts. In the context of classifying individuals by the number of their contacts, this model is similar to one used as a mean-field approximation to a network (Pastor-Satorras and Vespignani 2001). As for the homogeneous model in Sect. 2, we ignore demography. We let p_k denote the proportion of individuals with k daily contacts, and for convenience we use the probability generating function (P.G.F) formalism, $\Psi(x) = \sum_k p_k x^k$ to represent the probability distribution for the number of contacts. Here the sum is taken to be from $k = 0$ to the maximum number of contacts, say m. Note that $\Psi'(1) = \sum_k k p_k = \langle k \rangle$, which is the average number of contacts of an individual per day.

4.1 First wave dynamics

Let β denote the probability of transmission per infectious contact, and γ be the recovery rate. The dynamics are given by the equations

$$\begin{aligned} S_k' &= -\beta k S_k \frac{\sum_\ell \ell I_\ell}{\sum_\ell \ell p_\ell} \\ I_k' &= \beta k S_k \frac{\sum_\ell \ell I_\ell}{\sum_\ell \ell p_\ell} - \gamma I_k \\ R_k' &= \gamma I_k, \text{ for } k = 0, 1, 2, \ldots, m \end{aligned}$$

Since this is a closed system the population is constant (i.e., $\sum_k S_k + I_k + R_k = 1$). Furthermore, setting $S_k(0) \approx p_k$, $I_k(0) = p_k - S_k(0)$, $R_k = 0$, assures $S_k + I_k + R_k = p_k$ holds for all time. A straightforward application of the next generation matrix approach (van den Driessche and Watmough 2002) gives

$$\mathscr{R}_0^{(1)} = \frac{\beta}{\gamma} \frac{\sum_k k^2 p_k}{\langle k \rangle} = \frac{\beta}{\gamma} \left(\frac{Var[k]}{\langle k \rangle} + \langle k \rangle \right) = \frac{\beta}{\gamma} \frac{\langle k^2 \rangle}{\langle k \rangle}$$

This shows how $\mathscr{R}_0^{(1)}$ is related to the variance for the distribution of the number of contacts per day, as observed in Diekmann et al. (1990). Biologically, the average number of contacts for a contact is higher than the average of the population and is given by $\frac{\langle k^2 \rangle}{\langle k \rangle}$ (Feld 1991). Thus, $\mathscr{R}_0^{(1)}$ may be interpreted as the total number of infections caused by an initially infectious individual seeded by a randomly made interaction.

Now as we did before, we wish to derive the final state for the first wave to input as the initial conditions for the second wave dynamical equations. The equation for S_k' is linear in S_k and so the solution has the general form $S_k(t) = S_k(0) \exp\{-\int_0^t \beta k \frac{\sum_\ell \ell I_\ell}{\sum_\ell \ell p_\ell} dt\}$. Defining

$$\theta(t) := \exp\left(-\int_0^t \beta \frac{\sum_\ell \ell I_\ell}{\sum_\ell \ell p_\ell} dt \right)$$

gives

$$S_k(t) = S_k(0) \theta(t)^k$$

Thus, to obtain the final size of each compartment it is sufficient to calculate $\lim_{t \to \infty} \theta(t) = \theta_\infty$. Integrating the R_k equation gives

$$\int_0^\infty I_k dt = \frac{1}{\gamma} R_k(\infty) = \frac{1}{\gamma} (p_k - S_k(\infty)) = \frac{1}{\gamma} p_k (1 - \theta_\infty^k)$$

Substituting into $\theta(t)$ and simplifying gives

$$\theta_\infty = \exp\left\{-\frac{\beta}{\gamma}\left(1 - \frac{\theta_\infty \Psi'(\theta_\infty)}{\Psi'(1)}\right)\right\} \tag{3}$$

4.2 Second wave dynamics

We extend the first wave model in a straightforward manner to include the individuals who were infected and recovered in the previous year and segregate them by their number of contacts. We denote the fraction of degree k individuals that were previously infected as A_k, and define σ as in Sect. 3.2. The dynamics are given by

$$\begin{aligned}
S_k' &= -\beta k S_k \frac{\sum_\ell \ell I_\ell}{\sum_\ell \ell p_\ell} \\
A_k' &= -\sigma\beta k A_k \frac{\sum_\ell \ell I_\ell}{\sum_\ell \ell p_\ell} \\
I_k' &= \beta k(\sigma A_k + S_k)\frac{\sum_\ell \ell I_\ell}{\sum_\ell \ell p_\ell} - \gamma I_k \\
R_k' &= \gamma I_k, \text{ for } k = 0, 1, 2, \ldots, m
\end{aligned}$$

The initial conditions are $S_k(0) \approx p_k\theta_\infty^k$, $A_k(0) \approx p_k(1-\theta_\infty^k)$, $I_k(0) \approx 0$, $R_k(0) = 0$. The next generation matrix approach gives $\mathscr{R}^{(2)} = \frac{\beta}{\gamma}\frac{\sum_k((\sigma A_k(0)+S_k(0))k^2)}{\langle k\rangle}$. This can be rewritten in terms of θ_∞ as

$$\mathscr{R}^{(2)} = \frac{\beta}{\gamma}\frac{\sum_k(\sigma(1-\theta_\infty^k)+\theta_\infty^k)p_k k^2}{\langle k\rangle} \tag{4}$$

where θ_∞ is found by solving (3) Thus, once again, $\mathscr{R}^{(2)}$ is linearly dependent on σ. The threshold value σ_T for this multi-group model is found numerically for a given P.G.F. $\Psi(x)$ and fixed $\mathscr{R}_0^{(1)}$. For Fig. 1, we choose a time scale so that $\gamma = 1$, take $\mathscr{R}_0^{(1)} = 2$, approximately the value of $\mathscr{R}_0$ for the 1918 Spanish flu pandemic (Mills et al. 2004), and let $\frac{\langle k^2\rangle}{\langle k\rangle}$ range among 4,6,11. For the distributions we considered, namely, Poisson, discrete exponential (Exponential) and truncated power law (Power law), σ_T is less than the homogeneous mixing case; see Fig. 1. In addition, as $\frac{\langle k^2\rangle}{\langle k\rangle}$ increases, the multi-group $\mathscr{R}^{(2)}$ values approach the homogeneous $\mathscr{R}^{(2)}$ values. Furthermore, since $\mathscr{R}_0^{(1)}$ is in practice only an approximation, we test the sensitivity of our results by varying the value for $\mathscr{R}_0^{(1)}$ and computing σ_T; the results are summarized by Fig. 2.

5 Contact network models

5.1 The framework

Fixed contact networks are graphs in which nodes and edges represent individuals and contacts among individuals, respectively. Determining exact contact networks for

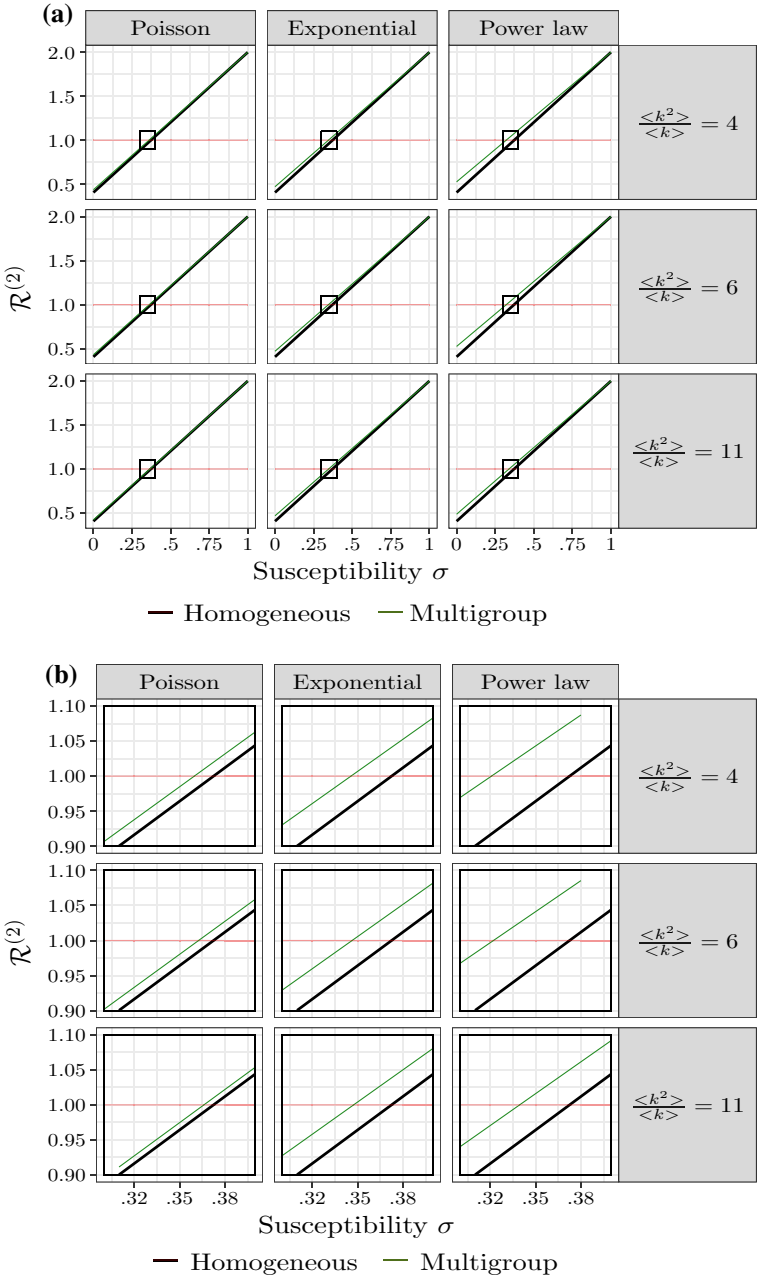

Fig. 1 **a** $\mathscr{R}^{(2)}$ is plotted against σ across various probability distribution families (columns) and $\frac{<k^2>}{<k>}$ (rows). For these numerics, models are parametrized so that $\mathscr{R}_0^{(1)} = 2$ and a timescale is chosen so that $\gamma = 1$. **b** The plots are expanded about the threshold $\mathscr{R}^{(2)} = 1$. For the probability distributions considered here, the multi-group model only slightly decreases σ_T, and the spread narrows as $\frac{<k^2>}{<k>}$ increases

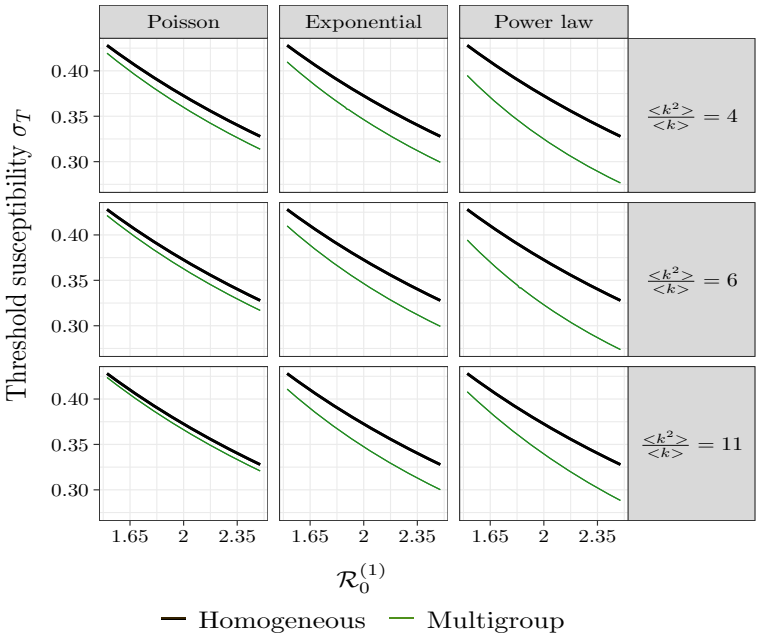

Fig. 2 Plot of σ_T versus $\mathscr{R}_0^{(1)}$ for fully homogeneous and multi-group models. Multi-group models were parametrized to follow Poisson, discrete exponential, and truncated power law distributions. Note that the multi-group models do not exhibit drastic reductions in σ_T compared to the fully homogeneous model

a large population is not a feasible task, however, network statistics such as size and degree probability distributions may be determined; see, for example, Pourbohloul et al. (2005). With the degree probability distribution, networks can be generated via the Molloy and Reed algorithm (Newman 2002). A very brief description of the algorithm is as follows. Assign to each node in a collection of edgeless nodes, a degree drawn from a given degree probability distribution. For the degree drawn, attach this number of half edges or 'stubs' to each node. Then choose two stubs uniformly and connect them to make an edge. We note that the sum of total degrees may not be even and/or loops may be possible in this construction; degrees may be re-drawn to fix the parity and loops are eliminated. Networks produced by this algorithm are generally referred to as Configuration Model (CM) networks and have the prescribed degree distribution, negligible clustering and negligible degree correlations. It is important to note that following a random edge from any given node, the probability of arriving at a node of a given degree is not only proportional to the density of such nodes in the network but also to the degree (i.e., densities being equal, it is more likely to arrive at higher degree nodes than lower degree nodes). This is in fact consistent with the real-world phenomenon where 'your friends have more friends than you do' (Feld 1991). Deterministic models of SIS and SIR type disease spread on CM networks have been developed; see, for example, House and Keeling (2010), Lindquist et al. (2011), Miller (2011), Newman (2002), Volz (2008). Most of these models were derived from seemingly different vantage points, differ in complexity, and differ in the physical

quantities they track during an epidemic, however they are intrinsically related and in some cases equivalent; see for example, House and Keeling (2010), Miller and Kiss (2014), Taylor and Kiss (2014). It is important to keep in mind that for all of the models just discussed, nodes or individuals undergo changes only in labeling, that is, individuals change in status as it relates to the disease states, however, the underlying contact network is assumed to stay fixed throughout the entire process. We note that the multi-group model described in Sect. 4 may be thought of as an extreme limit of the random network assumption where edges undergo fast rewiring (Kiss et al. 2017).

5.2 First wave dynamics

Even though the Volz–Miller formulation (Miller 2011; Volz 2008) has a much simpler form that the full pairwise SIR model (House and Keeling 2010), it is not straight forward to compute the infection state and degree distributions of susceptible and infected nodes after an epidemic, which is crucial for the dynamics of the second wave. We thus employ the pairwise SIR model (House and Keeling 2010) for the first wave dynamics. Note that this model is a direct extension of a simpler pairwise model (Keeling 1999), based on the same full pairwise approach developed in Eames and Keeling (2002). We assume the network is a CM network with degree PGF $\Psi(x) = \sum_k p_k x^k$. Here, β is the transmission rate across an edge and γ is the recovery rate for an infected node. Furthermore, $[X_k Y_j]$ denotes the fraction of edges connecting an X node of degree k with a Y node of degree j, where $X, Y \in \{S, I, R\}$. The dynamics of the pairwise model is given by the system

$$\begin{aligned}
\frac{d}{dt}[S_k I_j] &= -\beta[S_k I_j] + \beta[S_k S_j I] - \beta[I_j S_k I] - \gamma[S_k I_j] \\
\frac{d}{dt}[S_k S_j] &= -\beta([S_k S_j I] + [S_j S_k I]) \\
\frac{d}{dt}[S_k R_j] &= \gamma[S_k I_j] - \beta[I S_k R_j] \\
\frac{d}{dt}[R_k R_j] &= \gamma([I_j R_k] + [I_k R_j]) \\
\frac{d}{dt}S_k &= -\beta[S_k I]
\end{aligned}$$

Here, $I = \sum_\ell I_\ell$; for example, $[S_k S_j I] = \sum_\ell [S_k S_j I_\ell]$. Note that this system is not closed because we require the equation for $[X_j Y_k I]$, or the number of triples centered at node of type Y_k having a neighbor of type X_k and another infectious neighbor of any degree. Thus, a triple closure scheme $[X_j Y_k I] \approx \frac{[X_j Y_k][Y_k I](k-1)}{k Y_k}$ is applied (House and Keeling 2010) to arrive at the full system given by:

$$\frac{d}{dt}[S_k I_j] = -\beta[S_k I_j] + \beta\frac{[S_k S_j][S_j I](j-1)}{j S_j} - \beta\frac{[I_j S_k][S_k I](k-1)}{k S_k} - \gamma[S_k I_j] \tag{5}$$

$$\frac{d}{dt}[S_k S_j] = -\beta\left(\frac{[S_k S_j][S_j I](j-1)}{j S_j} + \frac{[S_k Sj][S_k I](k-1)}{k S_k}\right) \tag{6}$$

$$\frac{d}{dt}[S_k R_j] = \gamma[S_k I_j] - \beta\left(\frac{[IS_k][S_k R_j](k-1)}{kS_k}\right) \tag{7}$$

$$\frac{d}{dt}S_k = -\beta[S_k I] \tag{8}$$

Initial conditions are as follows:

$$[S_k I_j](0) = kS_k(0)\frac{I_j(0)}{\psi'(1)} = kp_k(1-\pi)\pi\frac{jp_j}{\psi'(1)} \tag{9}$$

$$[S_k S_j](0) = kS_k(0)\frac{jS_j(0)}{\psi'(1)} = kp_k(1-\pi)^2\frac{jp_j}{\psi'(1)} \tag{10}$$

$$[S_k R_j](0) = 0 \tag{11}$$

$$S_k(0) = p_k(1-\pi), \tag{12}$$

where π, $0 < \pi \ll 1$, is the probability a given node is infected at time 0. We note that these initial conditions satisfy a requirement of the CM assumption that the total number of edges connecting a degree k node with a degree j node or $[N_k N_j]$ satisfies

$$[N_k N_j] = \left(\frac{kp_k jp_j}{\psi'(1)}\right) \tag{13}$$

For SIR disease dynamics on a CM random static network with randomly chosen infectious individuals, the basic reproduction number for the first wave is given by Lindquist et al. (2011), Miller (2011), Newman (2002), Volz (2008)

$$\mathscr{R}_0^{(1)} = \frac{\beta}{\beta+\gamma}\left(\frac{\psi''(1)}{\psi'(1)}\right) \tag{14}$$

The term $\frac{\beta}{\beta+\gamma}$ is the transmission probability and $\frac{\psi''(1)}{\psi'(1)}$ is referred to as the average excess degree. i.e., the degree of a node found by following a random edge minus one for the edge being followed. Thus, $\mathscr{R}_0^{(1)}$ is the average number of infectious individuals caused by the typical infectious neighbour minus one to account for the contact who initially caused this infection. Contrast this with the distribution statistic $\frac{\langle k^2\rangle}{\langle k\rangle}$ used for multi-group models and note that $\frac{\langle k^2\rangle}{\langle k\rangle} = \frac{\psi''(1)}{\psi'(1)} + 1$.

5.3 Final state of first wave system

Here we obtain the final state of the first wave model, and use it as the initial conditions for the second wave of the disease. Existing literature provides the final fraction for each cohort of nodes; i.e., $S_k(\infty)$, $R_k(\infty)$ (note that $I_k(\infty) = 0$). This is done by showing equivalency between the system (5)–(8) with initial conditions (9)–(12) (Miller and Kiss 2014) and the edge based compartmental model (EBCM) approach (Miller 2011; Volz 2008). However, existing techniques do not go as far as evaluating

the final state for each pair type $[S_k S_j](\infty)$, $[R_k S_j](\infty)$ or $[R_k R_j](\infty)$. As such, this is the main goal of this section.

The first step is to define higher order variables from first wave dynamical variables. For $X, Y \in \{S, I, R\}$, we define $P_{X_k|Y_j}$ as the probability of arriving at a node in X of degree k, given that the edge originates from a node in Y of degree j, and it is given by

$$P_{X_k|Y_j} := \frac{[X_k Y_j]}{jY_j} \tag{15}$$

The dynamical equation for $P_{S_k|S_j}$ is found using (6) and (8) to give

$$\frac{d}{dt} P_{S_k|S_j} = \beta P_{S_k|S_j} P_{I|S_j} - \beta(k-1) P_{I|S_k} P_{S_k|S_j} \tag{16}$$

Note that here, $P_{I|S_j} = \sum_k P_{I_k|S_j}$. Equation (16) is linear in $P_{S_k|S_j}$, and the solution is given by

$$P_{S_k|S_j} = P_{S_k|S_j}(0) e^{-\beta \int_0^t \left((k-1)P_{I|S_k} - P_{I|S_j}\right) dt} \tag{17}$$

which is rewritten as

$$P_{S_k|S_j} = P_{S_k|S_j}(0) \left(e^{-\beta \int_0^t P_{I|S_k} dt}\right)^{k-1} \left(e^{\beta \int_0^t P_{I|S_j} dt}\right) \tag{18}$$

Define

$$\theta_k(t) := e^{-\beta \int_0^t P_{I|S_k} dt} \tag{19}$$

to simplify Eq. (18) as

$$P_{S_k|S_j} = P_{S_k|S_j}(0) \theta_k^{k-1} \theta_j^{-1} \tag{20}$$

Under the initial uniformity assumptions (9)–(11), θ_k is independent of k (Miller and Kiss 2014). In effect,

$$\theta(t) = e^{-\beta \int_0^t P_{I|S_k} dt} \tag{21}$$

for any k and (20) becomes

$$P_{S_k|S_j} = P_{S_k|S_j}(0) \theta^{k-2} \tag{22}$$

Furthermore, in Miller (2011), the limiting value for θ can be expressed by an implicit equation. Specifically, θ_∞ satisfies the implicit equation

$$\theta_\infty = \lim_{t\to\infty} \theta(t) = \frac{\gamma}{\beta+\gamma} + \frac{\beta}{\beta+\gamma} \left(\frac{\Psi'(\theta_\infty)}{\Psi'(1)}\right) \tag{23}$$

A solution for $\theta_\infty \in [0, 1)$ if it exists, is unique and can be computed numerically. Note that $\theta_\infty = 1$ is always a solution; corresponding to the disease free solution.

Solving (8) using (12), (15), and (19), it follows that

$$S_k(t) = p_k \theta(t)^k \tag{24}$$

when $\pi \approx 0$. Hence, the limiting value for S_k near the end of the first wave satisfies

$$S_k(\infty) = p_k \theta_\infty^k \tag{25}$$

as given in Miller (2011). This has an intuitive interpretation since $\theta(t)$ may be interpreted as the probability that there is no infectious transmission across a randomly selected edge leading to a susceptible node (Miller 2011). The negligible clustering assumption in the CM framework allows for the assumption of independence among edges. Thus, for a given degree k node, the probability that node remains susceptible by time t is equal to the probability there has been no transmission across any of its edges by time t, or $\theta(t)^k$.

Note that there are no infectious nodes remaining at the end of the first wave, thus

$$R_k(\infty) = p_k - S_k(\infty) = p_k(1 - \theta_\infty^k)$$

In addition, (22) along with (10) and (12) and $\pi \approx 0$ gives

$$P_{S_k|S_j}(\infty) \approx \frac{k p_k}{\psi'(1)} \theta_\infty^{k-2} \tag{26}$$

Finally, using (15)

$$[S_k S_j](\infty) \approx \left(\frac{j p_j k p_k}{\psi'(1)} \right) \theta_\infty^{k+j-2} \tag{27}$$

This quantity has a nice interpretation. At the end of the first wave, pick an arbitrary edge of type $[N_k N_j]$ and note that so long as the disease has not crossed towards either node from any of their other neighbors, the edge is guaranteed to be of type $[S_k S_j]$. The S_k node has $k - 1$ remaining edges across which the disease has not crossed: occurring with probability θ_∞^{k-1}. Similarly, the degree j node is susceptible with probability θ_∞^{j-1}. Finally, recalling (13), (27) follows.

The calculation giving that

$$[S_k R_j](\infty) \approx \left(\frac{\gamma}{\beta + \gamma} \right) \left(\frac{j p_j k p_k}{\psi'(1)} \right) (1 - \theta_\infty^{j-1}) \theta_\infty^{k-1} \tag{28}$$

is shown in the "Appendix". Here, we restrict the discussion to an intuitive interpretation of this expression. Take a random edge of type $[N_k N_j]$ at the end of the first wave but prior to the start of the second wave. Ignoring transmissions across this edge (note that if a transmission did occur across the edge, then the final status $[S_k R_j](\infty)$ is not possible) the degree k node remained susceptible with probability θ_∞^{k-1} and the

Table 1 Novel expressions for the final state of the network SIR pairwise model. They are given in terms of θ_∞ and degree distribution parameters

Limiting values	How to compute
$S_k(\infty)$	$p_k\theta_\infty^k$
$R_k(\infty)$	$p_k(1-\theta_\infty^k)$
$[S_kS_j](\infty)$	$\left(\frac{jp_jkp_k}{\psi'(1)}\right)\theta_\infty^{k+j-2}$
$[S_kR_j](\infty)$	$\left(\frac{\gamma}{\beta+\gamma}\right)\left(\frac{jp_jkp_k}{\psi'(1)}\right)(1-\theta_\infty^{j-1})\theta_\infty^{k-1}$
$[R_kR_j](\infty)$	$\left(\frac{jp_jkp_k}{\psi'(1)}\right)\left(1-\left(\frac{\gamma}{\beta+\gamma}\right)\left((1-\theta_\infty^{j-1})\theta_\infty^{k-1}+(1-\theta_\infty^{k-1})\theta_\infty^{j-1}\right)-\theta_\infty^{k+j-2}\right)$

degree j node became infectious with probability $1-\theta_\infty^{j-1}$. Finally, the degree k node remained susceptible only if there was no transmission across the edge itself during the infectious period for the degree j node; this occurs with probability $\frac{\gamma}{\gamma+\beta}$.

Calling upon the conservation of mass equation

$$\begin{aligned}[N_kN_j] = {} & [S_kS_j](t)+[S_kI_j](t)+[I_kS_j](t)+[I_kI_j](t)+[S_kR_j](t) \\ & +[R_kS_j](t)+[I_kR_j](t)+[R_kI_j](t)+[R_kR_j](t)\end{aligned} \tag{29}$$

and noting that there are no edges with an infectious node remaining at the end of the first wave and prior to the second wave, then (29) simplifies to:

$$[N_kN_j](\infty) = [S_kS_j](\infty)+[S_kR_j](\infty)+[R_kS_j](\infty)+[R_kR_j](\infty) \tag{30}$$

Here, $[R_kS_j](\infty)$ is given by applying a symmetric argument to (28). Finally (30) gives $[R_kR_j](\infty)$ as

$$[R_kR_j](\infty) = [N_kN_j](\infty)-[R_kS_j](\infty)-[S_kR_j](\infty)-[S_kS_j](\infty)$$

where $[N_kN_j](\infty)$ is given by (13). Thus, the final state for the first wave system is fully derived and is summarized in Table 1.

5.4 Second wave dynamics

At onset of the second wave, the recovered individuals in R_k are partially susceptible to re-infection; we label these individuals as A_k. The susceptibility of these individuals is reduced by a factor $\sigma \in [0,1]$. Individuals in S_k remain in S_k. Figure 3 shows the possible state transitions. From the final state of the first wave the second wave variables have initial conditions (with no disease present) $S_k(0) = p_k\theta_\infty^k$, $A_k(0) = p_k(1-\theta_\infty^k)$.

We are now ready to derive the SAIR network model analogously to the model derived in Miller (2011). The probability that an individual initially in S_k remains susceptible by time t, is the probability that the disease has not been transmitted across any of its k edges. We define θ_{S_k} as the probability that the disease has not been transmitted across an edge that leads to an S_k node at time t. A random network

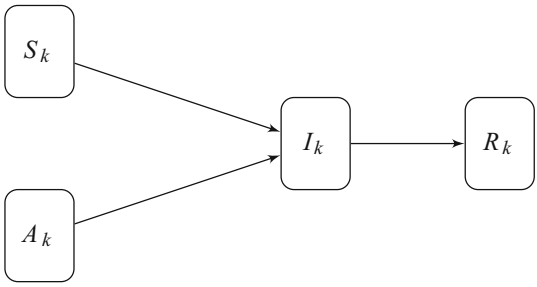

Fig. 3 State transitions for degree k node in the dynamics for the second wave. Here S_k denotes the fraction of degree k nodes that escaped infection in the first wave and have not been infected in the second wave, A_k is the fraction of degree k nodes that were infected and recovered in the first wave but have not been infected in the second wave

generated by the CM model has negligible clustering, thus edges are independent and the probability that a node in S_k is susceptible at time t is $\theta_{S_k}^k$. Define θ_{A_k} in a similar fashion and thus the probability an individual in A_k remains susceptible by time t is $\theta_{A_k}^k$. We define ϕ_{S_k}, ϕ_{A_k} as the fraction of edges leading to a S_k, A_k node and also connected to an infectious node at time t. Note that these edges are also in θ_{S_k} and θ_{A_k}, respectively. Hence,

$$\frac{d}{dt}\theta_{S_k} = -\beta\phi_{S_k} \tag{31}$$

$$\frac{d}{dt}\theta_{A_k} = -\sigma\beta\phi_{A_k} \tag{32}$$

The dynamical equations for ϕ_{S_k}, ϕ_{A_k} are required. We let h_{S_k} be the probability the node reached following a θ_{S_k} edge (out of the S_k node) has not been infected at time t. This probability depends on whether or not the node reached by following this edges was originally an A or S node. At the onset of the second wave, a node reached by following a θ_{S_k} edge is in S_j with probability

$$P_{S_j|S_k}(0) := \frac{[S_j S_k](\infty)}{k S_k(\infty)} \tag{33}$$

Note that values $[S_k S_j](\infty)$, and $[S_k](\infty)$ are read from Table 1, and that $P_{S_k|S_j}(0)$ differs from the value used in (17), which refers to the probability of reaching an S_j node prior to the first wave. Furthermore, the neighbor node reached remains in S_j if none of its $j-1$ other neighbors has transmitted the disease to it. Thus, the probability the neighbor reached is in S_j at time t is $P_{S_j|S_k}(0)\theta_{S_j}(t)^{j-1}$. Correspondingly, the probability that a node reached at time t is in A_j has probability $P_{A_j|S_k}(0)\theta_{A_j}^{j-1}$. Thus,

$$h_{S_k} = \sum_j \left(P_{A_j|S_k}(0)\theta_{A_j}^{j-1} + P_{S_j|S_k}(0)\theta_{S_j}^{j-1} \right)$$

Furthermore, in an analogous manner, we define

$$h_{A_k} = \sum_j \left(P_{A_j|A_k}(0)\theta_{A_j}^{j-1} + P_{S_j|A_k}(0)\theta_{S_j}^{j-1} \right)$$

Table 2 Second wave correlations computed using Table 1 and (15)

Correlations	How to compute
$P_{S_j\|A_k}(0)$	$\left(\frac{\gamma}{\beta+\gamma}\right)\frac{jp_j(1-\theta_\infty^{k-1})\theta_\infty^{j-1}}{(1-\theta_\infty^k)\psi'(1)}$
$P_{A_j\|S_k}(0)$	$\left(\frac{\gamma}{\beta+\gamma}\right)\frac{jp_j(1-\theta_\infty^{j-1})}{\theta_\infty\psi'(1)}$
$P_{A_j\|A_k}(0)$	$\frac{jp_j}{(1-\theta_\infty^k)\psi'(1)}\left(1-\left(\frac{\gamma}{\beta+\gamma}\right)\left((1-\theta_\infty^{j-1})\theta_\infty^{k-1}+(1-\theta_\infty^{k-1})\theta_\infty^{j-1}\right)-\theta_\infty^{k+j-2}\right)$
$P_{S_j\|S_k}(0)$	$\frac{\theta_\infty^{j-2}jp_j}{\psi'(1)}$

The rate at which edges enter ϕ_{S_k} is equal in magnitude to the rate at which neighbors reached by following a θ_{S_k} edge become infectious. Thus, ϕ_{S_k} is increased at a rate $-\frac{d}{dt}h_{S_k}(t)$. Furthermore, edges in ϕ_{S_k} leave when transmission occurs across the edge or when the infectious node recovers. Since the dynamics for ϕ_{A_k} are similar, the equations for ϕ_{S_k} and ϕ_{A_k} may now be written as

$$\frac{d}{dt}\phi_{S_k} = -(\beta+\gamma)\phi_{S_k} - \frac{d}{dt}h_{S_k}$$

and

$$\frac{d}{dt}\phi_{A_k} = -(\sigma\beta+\gamma)\phi_{A_k} - \frac{d}{dt}h_{A_k}$$

Thus,

$$\frac{d}{dt}\phi_{S_k} = -(\beta+\gamma)\phi_{S_k} + \sum_j (j-1)\left(\sigma\beta P_{A_j|S_k}(0)\theta_{A_j}^{j-2}\phi_{A_j} + \beta P_{S_j|S_k}(0)\theta_{S_j}^{j-2}\phi_{S_j}\right) \quad (34)$$

$$\frac{d}{dt}\phi_{A_k} = -(\sigma\beta+\gamma)\phi_{A_k} + \sum_j (j-1)\left(\sigma\beta P_{A_j|A_k}(0)\theta_{A_j}^{j-2}\phi_{A_j} + \beta P_{S_j|A_k}(0)\theta_{S_j}^{j-2}\phi_{S_j}\right) \quad (35)$$

with initial conditions:

$$\theta_{S_k}(0) = \theta_{A_k}(0) = 1 \quad (36)$$

$$\phi_{S_k}(0) = \phi_{A_k}(0) \approx 0 \quad (37)$$

We remark that these initial conditions may be interpreted as uniformity in the distribution of initial nodes infected among all network nodes. From Table 2, $P_{A_j|S_k}(0)$ and $P_{S_j|S_k}(0)$ show that these values do not depend on k, therefore, the equations for ϕ_{S_k} are independent of k. In other words, this means that knowing that a node was in S at the beginning of the second wave tells us as much information about its neighbors as possible (i.e., knowing its degree is irrelevant). Therefore, we drop the subscript k from $P_{A_j|S_k}(0)$, $P_{S_j|S_k}(0)$, and ϕ_{S_k}. The reproduction number for this system can be

computed as the spectral radius of the next generation matrix (van den Driessche and Watmough 2002). That is

$$\mathscr{R}^{(2)} = \rho(FV^{-1}) \tag{38}$$

where we order the variables associated with disease states as $\{\phi_{A_1}, \phi_{A_2}, \ldots \phi_{A_n}, \phi_S\}$ from (35) and (34). Thus, the F and V^{-1} matrices are $(n+1) \times (n+1)$ with

$$V^{-1} = diag\left(\frac{1}{\sigma\beta+\gamma}, \ldots, \frac{1}{\sigma\beta+\gamma}, \frac{1}{\beta+\gamma}\right)$$

and

$$F = \begin{pmatrix} 0 & \sigma\beta P_{A_2|A_1}(0) & \ldots & (n-1)\sigma\beta P_{A_n|A_1}(0) & \beta\sum_j (j-1)P_{S_j|A_1}(0) \\ 0 & \sigma\beta P_{A_2|A_2}(0) & \ldots & (n-1)\sigma\beta P_{A_n|A_2}(0) & \beta\sum_j (j-1)P_{S_j|A_2}(0) \\ 0 & \sigma\beta P_{A_2|A_3}(0) & \ldots & (n-1)\sigma\beta P_{A_n|A_3}(0) & \beta\sum_j (j-1)P_{S_j|A_3}(0) \\ \vdots & \vdots & & \vdots & \vdots \\ 0 & \sigma\beta P_{A_2|S}(0) & \ldots & (n-1)\sigma\beta P_{A_n|S}(0) & \beta\sum_j (j-1)P_{S_j|S}(0) \end{pmatrix}$$

Hence FV^{-1} is

$$\begin{pmatrix} 0 & \frac{\sigma\beta}{\sigma\beta+\gamma} P_{A_2|A_1}(0) & \ldots & (n-1)\frac{\sigma\beta}{\sigma\beta+\gamma} P_{A_n|A_1}(0) & \sum_j \frac{\beta}{\beta+\gamma}(j-1)P_{S_j|A_1}(0) \\ 0 & \frac{\sigma\beta}{\sigma\beta+\gamma} P_{A_2|A_2}(0) & \ldots & (n-1)\frac{\sigma\beta}{\sigma\beta+\gamma} P_{A_n|A_2}(0) & \sum_j \frac{\beta}{\beta+\gamma}(j-1)P_{S_j|A_2}(0) \\ 0 & \frac{\sigma\beta}{\sigma\beta+\gamma} P_{A_2|A_3}(0) & \ldots & (n-1)\frac{\sigma\beta}{\sigma\beta+\gamma} P_{A_n|A_3}(0) & \sum_j \frac{\beta}{\beta+\gamma}(j-1)P_{S_j|A_3}(0) \\ \vdots & \vdots & & \vdots & \vdots \\ 0 & \frac{\sigma\beta}{\sigma\beta+\gamma} P_{A_2|S}(0) & \ldots & (n-1)\frac{\sigma\beta}{\sigma\beta+\gamma} P_{A_n|S}(0) & \sum_j \frac{\beta}{\beta+\gamma}(j-1)P_{S_j|S}(0) \end{pmatrix}$$

with the conditional probabilities given in Table 2. Note that from this matrix, $\mathscr{R}^{(2)}$ is a function of σ. Without a simple expression for $\rho(FV^{-1})$, for Fig. 4 we compute $\mathscr{R}^{(2)}$ numerically and compare with Fig. 1 for fixed $\mathscr{R}_0^{(1)} = 2$. Furthermore, as done in the previous section, we allow $\mathscr{R}_0^{(1)}$ to vary and numerically compute the susceptibility threshold σ_T. Note that the distinct expressions for $\mathscr{R}_0^{(1)}$ among homogeneous, multi-group, and network models means that the transmission rate β has to differ so that $\mathscr{R}_0^{(1)}$ is constant among all models. For multi-group and network models, we compare among Poisson, discrete exponential, and power law probability distributions with varying average excess degree. Figure 4 shows how networks tend to have a lower susceptibility threshold, σ_T, than multi-group models parametrized with identical probability distributions. As discussed earlier, multi-group models in turn tend to have slightly lower σ_T than the fully homogeneous model. The order of reduction in σ_T for network models is significant relative to the respective σ_T value for the multi-group models and this relation holds for a wide interval of possible basic reproduction numbers for the first wave as shown by Fig. 5. Lastly, numerics suggest that as the average excess degree is increased, the network curves approach the fully homogeneous mixing line.

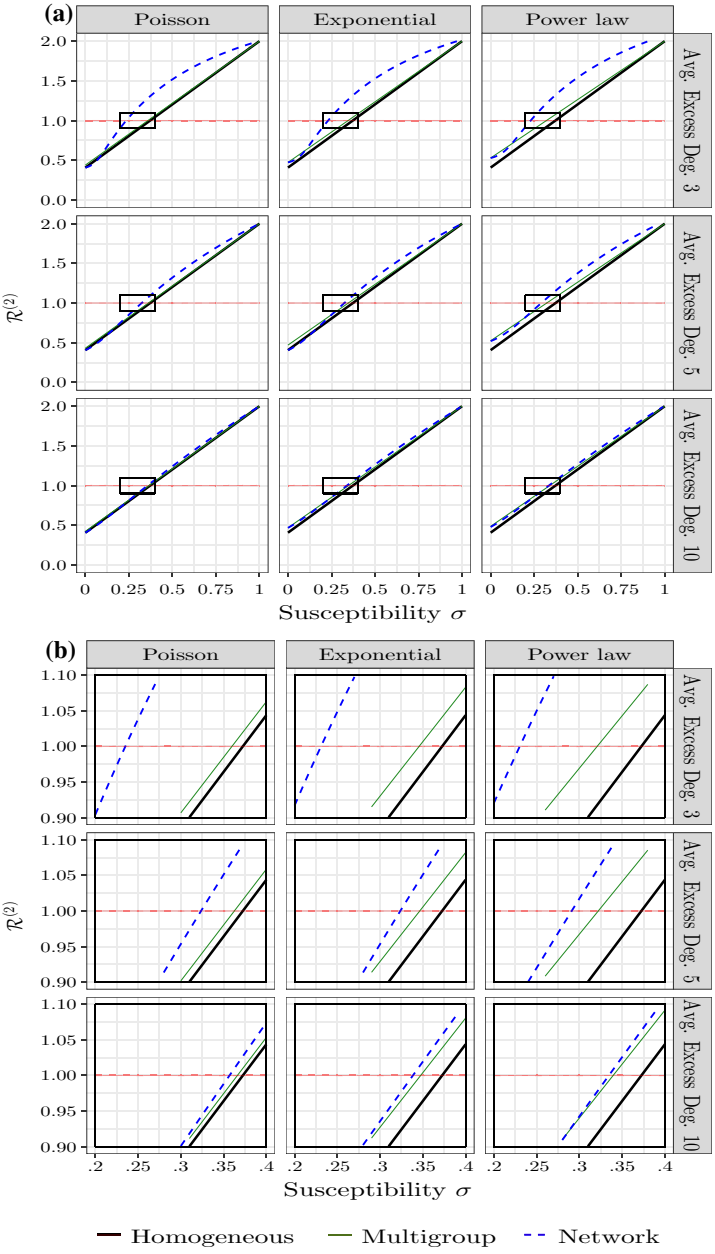

Fig. 4 **a** $\mathscr{R}^{(2)}$ is plotted against susceptibility (σ) for network(dashed), multi-group(solid), and homogeneous model(solid, thick). Here, $\mathscr{R}_0^{(1)} = 2$ and a timescale has been chosen so that $\gamma = 1$. **b** The plots are expanded about the threshold $\mathscr{R}^{(2)} = 1$. For network models and and a degree distribution with a low average excess degree, $\mathscr{R}^{(2)}$ increases non-linearly with σ; this leads to $\mathscr{R}_0 > 1$ at significantly lower levels of σ when compared to random mixing models. As the average excess degree (Avg. Excess Deg., i.e., $\frac{\langle k^2 \rangle}{\langle k \rangle} - 1$) increases (down a column), all models approach the values for the homogeneous SIR model

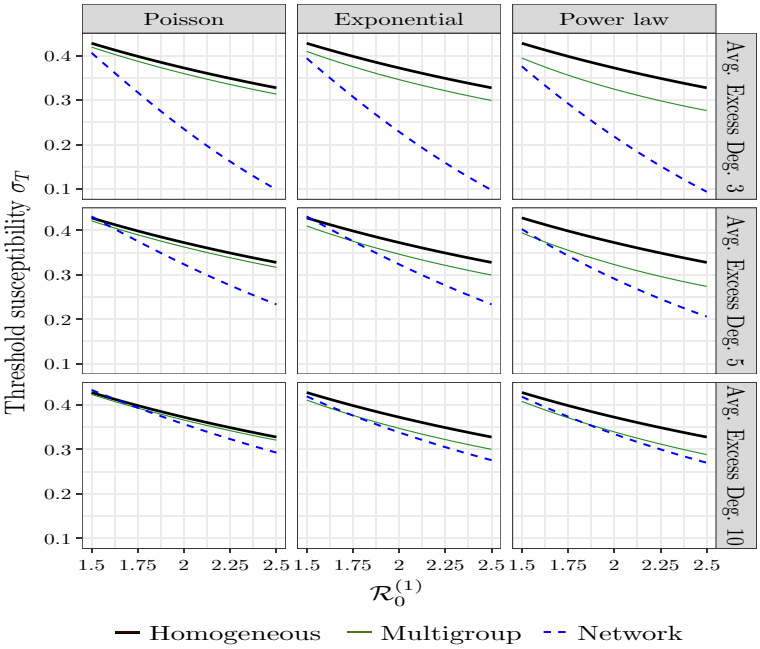

Fig. 5 As in Figure 2, we plot the susceptibility threshold (σ_T) versus. $\mathscr{R}_0^{(1)}$. Here, we include the network models along with the random mixing models. In general, σ_T is lower for network models than the random mixing models for a wide range of $\mathscr{R}_0^{(1)}$ values. The gap increases with either increasing $\mathscr{R}_0^{(1)}$ or lowering the average excess degree (Avg. Excess Deg., i.e., $\frac{\langle k^2\rangle}{\langle k\rangle} - 1$)

The choices for distributions and average excess degrees give a good sampling of distributions and the parameterizations thereof. However, once a population of interest is identified, a probability distribution should be inferred and the numerical work should be repeated for an accurate estimation for σ_T. Notwithstanding, the numerics do seem to suggest that the spread between σ_T among random mixing and contact network models tends to be most pronounced as $\mathscr{R}_0^{(1)}$ increases, and on degree distributions with a smaller average excess degree. Figure 4 shows how networks tend to have a lower susceptibility threshold, σ_T, than multi-group models parametrized with identical probability distributions. In turn, multi-group models tend to have slightly lower σ_T than the fully homogeneous model. The order of reduction in σ_T for network models is significant relative to the respective σ_T value for the multi-group models and this relation holds for a wide interval of basic reproduction numbers for the first wave as shown by Fig. 5.

To test the accuracy of the predicted σ_T value, we ran stochastic network simulations on networks with average excess degree set at 3 and $\mathscr{R}_0^{(1)} = 2$; see Fig. 6. From Fig. 5, σ_T for Poisson, discrete exponential and power law is approximately, 0.235, 0.228 and 0.230 respectively. Thus, the simulations suggests that the model accurately predicts the point where a paradigm shift occurs. This confirms a significant reduction in the antigenic drift required for a recurrence event in network models relative to any of the random mixing models where $0.33 < \sigma_T < 0.38$.

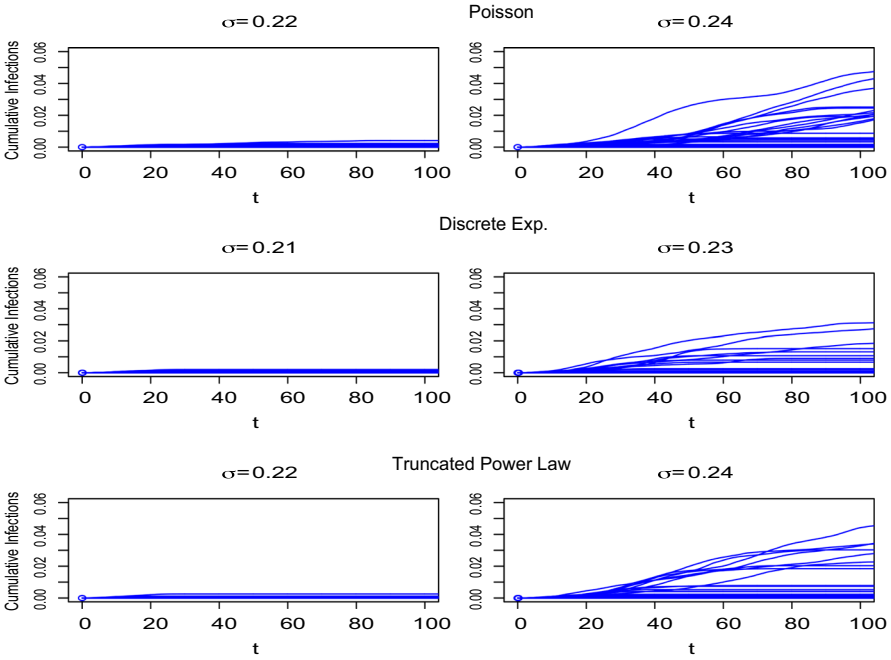

Fig. 6 Simulated cumulative cases versus time in the second wave epidemic on Configuration-model networks (500,000 nodes) with Poisson, discrete exponential and truncated power law distributions and average excess degree set at 3. Our model predicts $\sigma_T = 0.235, 0.228, 0.230$ for Poisson, discrete exponential and truncated power law respectively. After simulating a first wave with $\mathscr{R}_0^{(1)} = 2$, we ran 250 simulations of the second wave for each σ value slightly below and above the theoretically predicted σ_T value. Results show that above the threshold there is a clear binary outcome: either a single infectious individual does not cause an epidemic or an outbreak occurs. This shows that our model accurately predicts the point of regime change

6 Discussion

The 2009 H1N1 pandemic and the subsequent flu seasons presented a somewhat enigmatic phenomenon. While the dominant 2009 H1N1 strain that was responsible for a majority of the cases did not undergo significant or detectable antigenic change (Klein et al. 2014), closely related variants caused outbreaks in subsequent flu seasons; as experienced in Morocco, England, Argentina, Singapore, and Greece (Barr et al. 2010; El Rhaffouli et al. 2014; Hoschler et al. 2012; Russo et al. 2014). This has inevitably led to the formulation of biological and molecular hypothesis to explain this phenomenon. In this paper, a minimalistic theoretical network model offers a framework in which a post pandemic recurrence in a given geographical location is possible even after relatively little antigenic drift.

We also point out that the network models studied here make some simplistic assumptions that must be considered before directly inferring results to influenza A spreading on a real human contact network. First of all, Configuration Model networks provide a tractable handle on contact network structures; however, they do not

incorporate clustering or degree correlations, which are expected to be a characteristic of real contact networks. Explorations on how these factors affect the susceptibility threshold merits its own investigation. Furthermore, the network models presented here are fixed while real contact network would not be. However, we expect this to be reasonable assumption due to the difference in timescales between the dynamics of a real contact network and that of the first and second wave of influenza A. Finally, we presented results for common degree distributions and various parameterizations, yet these distributions were chosen for purely demonstrative purposes. For a more accurate estimation of σ_T, proper degree distributions should be inferred based on the population in question. A couple of natural questions and insights also follow from this work. Following the first wave, disease dynamics induce correlations among states and degrees. Numerics not presented here seem to suggest that the second wave is slightly more likely to occur in a network where these correlations are ignored and the A and S nodes are wired in a CM-type manner. This suggests that as the network undergoes slow rewiring between the first and second waves, the invasion risk of a variant pandemic strain grows. Furthermore, it is reasonable to ask the extent to which different final sizes between networks and random mixing models for a given $\mathscr{R}_0^{(1)}$ contribute to the network susceptibility to the variant strain. We note that CM networks with Poisson degree distribution have final sizes that correspond to that of the homogeneous random mixing assumption (Brauer et al. 2008), however they have different susceptibility thresholds ($\sigma_T \approx 0.24$ vs. $\sigma_T \approx 0.37$). Thus, our findings suggest the susceptibility of contact networks to re-invasion is driven by relatively fixed contacts, and the fact that each individual's contacts are different, rather than differences in final sizes of the first wave given $\mathscr{R}_0^{(1)}$.

7 Conclusion

Infectious disease modellers are often faced with the challenge of deciding which features to include and which to exclude. If too many simplifying assumptions are made, then the model might fail to produce accurate results representing reality. In this paper we have shown that host population structure is an important feature to include in influenza models with implications for both control and evolutionary theory of influenza A. Specifically, we have shown that a population modelled by a random contact CM network may be drastically more vulnerable to the recurrence of an influenza strain following an initial pandemic relative to populations modelled under the random mixing assumption. Under the latter assumption, an increase in susceptibility of previously infected individuals caused by antigenic drift results in a linear increase of the reproduction number following the pandemic ($\mathscr{R}^{(2)}$). We showed that this holds true even when heterogeneity in the number of contacts among individuals is considered while maintaining the random mixing assumption. This linear dependence between $\mathscr{R}^{(2)}$ and susceptibility requires an unrealistically large amount of antigenic drift for a recurrence of a novel influenza strain to be possible. This is unrealistic, since for example, from the time of emergence in 2009–2014, it appears that the A(H1N1)pmd09 pandemic strain has undergone a fairly limited amount of

antigenic change (Klein et al. 2014). Furthermore, it has been estimated that the value for the reduction in cross immunity is at the level of around 25% per annum (Kucharski et al. 2015).

We considered models that incorporate a network structure where individuals interact with a fixed set of contacts and the number of contacts varies from individual to individual. We extracted correlations induced by the first wave dynamics and formulated a CM random network model for the second wave. We showed numerically that for realistic parameterizations and common network degree distributions, $\mathscr{R}^{(2)}$ depends non-linearly on σ. We demonstrated that the reduction in the required antigenic drift for a recurrence on a network can be dramatically less than models that make the random mixing assumption.

This suggests that host population contact structure may be an important factor in the establishment of a novel influenza strain Furthermore, it suggests that stable contacts, such as family members, classmates, and coworkers may be crucial for the spread of influenza in human populations.

Acknowledgements The research of Junling Ma and P. van den Driessche is partially supported by NSERC Discovery Grants and the research of Sanling Yuan is supported by the Natural Science Foundation of China Grant (11671260). We thank the University of Victoria for financial support of J. M. Jaramillo during his graduate studies. We thank the two anonymous referees for helpful comments and references.

Appendix

In this "Appendix" we derive $[S_k R_j](\infty)$ as given in (28). Our starting point is the differential equation for $[S_k I_j]$ given by (5) and initial condition (9). Defining $P_{I|S_j} := \frac{[S_j I]}{jS_j}$, and substituting into (5) gives

$$\frac{d}{dt}[S_k I_j] = \beta[S_k S_j]P_{I|S_j}(j-1) - [S_k I_j](\beta+\gamma) - \beta P_{I|S_k}[S_k I_j](k-1)$$

multiplying by an integrating factor and simplifying yields

$$\frac{d}{dt}\left([S_k I_j]e^{\int_0^t((\beta+\gamma)+\beta P_{I|S_k}(k-1))d\tau}\right) = \beta[S_k S_j]P_{I|S_j}(j-1)e^{\int_0^t((\beta+\gamma)+\beta P_{I|S_k}(k-1))d\tau}$$

Recall the definition for θ_k given in (19) and the result from Miller and Kiss (2014) that under the assumption of randomly selected initially infectious individuals, θ_k is independent of its subscript. Thus, the previous equation after integrating and simplification yields

$$\begin{aligned}[S_k I_j](t) &= \left(\int_0^t \beta[S_k S_j](a)P_{I|S_j}(a)(j-1)\theta^{-(k-1)}(a)e^{(\beta+\gamma)a}da\right)\theta^{k-1}e^{-(\beta+\gamma)t} \\ &\quad + [S_k I_j](0)\theta^{k-1}e^{-(\beta+\gamma)t} \\ &= \left(\frac{1}{c}\right)\left(\int_0^t \beta(\theta(a)^{k+j-2}P_{I|S_j}(a)e^{(\beta+\gamma)a}\theta(a)^{-(k-1)}da\right)\theta^{k-1}e^{-t(\beta+\gamma)}\end{aligned}$$

$$
\begin{aligned}
&+ [S_k I_j](0)\theta^{k-1}e^{-(\beta+\gamma)t} \\
&= \left(\frac{1}{c}\right)\left(\int_0^t \beta(j-1)P_{I|S_j}\theta(a)^{j-1}e^{(\beta+\gamma)a}da + c[S_k I_j](0)\right)\theta(t)^{k-1}e^{-(\beta+\gamma)t} \\
&= \left(\frac{1}{c}\right)\left(\int_0^t -\frac{d}{da}\left(\theta(a)^{j-1}\right)e^{(\beta+\gamma)a}da + c[S_k I_j](0)\right)\theta(t)^{k-1}e^{-(\beta+\gamma)t} \quad (39)
\end{aligned}
$$

We have used (24) and (27) to substitute for $[S_k S_j](a)$ and

$$c = \left(\frac{jp_j kp_k}{\psi'(1)}\right)^{-1}$$

At this point we leave the current expression for $[S_k I_j](t)$ and turn to calculate $[S_k R_j](t)$. Recall from (7) that

$$\frac{d}{dt}[S_k R_j](t) = \gamma[S_k I_j] - \beta[S_k R_j]P_{I|S_k}(k-1)$$

Multiplying by an integrating factor gives

$$\frac{d}{dt}\left([S_k R_j](t)e^{\int_0^t \beta P_{I|S_k}(k-1)}\right) = \gamma[S_k I_j]e^{\int_0^t \beta P_{I|S_k}(k-1)} = \gamma[S_k I_j]\theta(t)^{-(k-1)}$$

Integrating and using (11) gives

$$[S_k R_j](t) = \gamma\left(\int_0^t [S_k I_j](\tau)\theta(\tau)^{-(k-1)}d\tau\right)\theta(t)^{(k-1)}$$

Substituting (39) yields

$$[S_k R_j](t) = \frac{\gamma}{c}\left(\int_0^t F_j(\tau)e^{-(\beta+\gamma)\tau}d\tau\right)\theta(t)^{(k-1)} \quad (40)$$

where

$$
\begin{aligned}
F_j(\tau) &:= \int_0^\tau -\frac{d}{da}\left(\theta(a)^{j-1}\right)e^{(\beta+\gamma)a}da + c[S_k I_j](0) \\
&= \int_0^\tau -\frac{d}{da}\left(\theta(a)^{j-1}\right)e^{(\beta+\gamma)a}da + \pi(1-\pi)
\end{aligned}
$$

by substituting initial conditions (9). The groundwork has now been set to extract an expression for $[S_k R_j](\infty)$.

Proposition 1 *Equation* (28)*, i.e.,*

$$[S_k R_j](\infty) = \left(\frac{\gamma}{\beta+\gamma}\right)\left(\frac{jp_j kp_k}{\psi'(1)}\right)\left(1-\theta_\infty^{j-1}\right)\theta_\infty^{(k-1)}$$

Proof From the calculations above let

$$G_j = F_j e^{-(\beta+\gamma)t}$$

so that

$$G_j' = F_j' e^{-(\beta+\gamma)t} - (\beta+\gamma) F_j e^{-(\beta+\gamma)t}$$

Noting that

$$F_j' = -\frac{d}{dt}\left(\theta(t)^{j-1}\right) e^{(\beta+\gamma)t}$$

and after integration and substitution

$$\int_0^t G_j' dt = \int_0^t -\frac{d}{dt}\left(\theta(t)^{j-1}\right) dt - \int_0^t (\beta+\gamma) F_j e^{-(\beta+\gamma)t} dt$$

Letting $t \to \infty$ gives

$$G_j(\infty) - G_j(0) = -\theta(t)^{j-1}|_0^\infty - (\beta+\gamma)\int_0^\infty F_j e^{-(\beta+\gamma)t} dt$$

That is,

$$1 - \theta_\infty^{j-1} - (\beta+\gamma)\int_0^\infty F_j e^{-(\beta+\gamma)t} dt = 0 \tag{41}$$

To see why the left hand side is essentially zero requires some work. First note that $G_j(0) \approx 0$ follows immediately from the fact that $F_j(0) \approx 0$ for small enough π. To see why $G_j(\infty) = 0$, we must consider two cases; F_j' is positive, thus F_j either converges to some value or diverges to positive infinity. In the first case it easily follows that

$$\lim_{t\to\infty} G_j = 0$$

In the second case, we apply L'Hôpital's rule, which gives

$$\lim_{t\to\infty} G_j = \lim_{t\to\infty} \frac{F_j'}{(\beta+\gamma)e^{(\beta+\gamma)t}} = \lim_{t\to\infty} \frac{-\frac{d}{dt}\left(\theta(t)^{j-1}\right)}{(\beta+\gamma)} = 0$$

since $\frac{d}{dt}\theta(t) \to 0$ as $t \to \infty$ which is evident from the fact that $P_{I|S_k} \to 0$ and differentiating θ from (21). From (41),

$$\frac{1-\theta_\infty^{j-1}}{(\beta+\gamma)} = \int_0^\infty F_j e^{-(\beta+\gamma)t} dt \tag{42}$$

Finally, substituting (42) into (41) gives the required result. □

References

Andreasen V (2003) Dynamics of annual influenza A epidemics with immuno-selection. J Math Biol 46:504–536

Andreasen V, Lin J, Levin S (1997) The dynamics of cocirculating influenza strains conferring partial cross-immunity. J Math Biol 35:825–842

Asaduzzaman S, Ma J, van den Driessche P (2015) The coexistence or replacement of two subtypes of influenza. Math Biosci 270(Part A):1–9

Barr I, Cui L, Komadina N, Lee R, Lin R, Deng Y, Caldwell N et al (2010) A new pandemic influenza A (H1N1) genetic variant predominated in the winter 2010 influenza season in Australia, New Zealand and Singapore. Eurosurveillance 15(42):19,692

Besselaar TG, Botha L, McAnerney JM, Schoub BD (2004) Antigenic and molecular analysis of influenza a (H3N2) virus strains isolated from a localised influenza outbreak in South Africa in 2003. J Med Virol 73(1):71–78

Both G, Sleigh M, Cox N, Kendal A (1983) Antigenic drift in influenza virus H3 Hemagglutinin from 1968 to 1980: multiple evolutionary pathways and sequential amino acid changes at key antigenic sites. J Virol 48:52–60

Brauer F, van den Driessche P, Wu J (eds) (2008) Mathematical epidemiology, vol 1945. Springer, Berlin

Bush R, Fitch W, Bender C, Cox N (1999) Positive selection on the H3 Hemagglutinin gene of human influenza virus a. Mol Biol 16:1457–1465

Carrat F, Flahault A (2007) Influenza vaccine: the challenge of antigenic drift. Vaccine 25:39–40

Casagrandi R, Bolzoni L, Levin S, Andreasen V (2006) The SIRC model and influenza A. Math Biosci 200:152–169

Chatterjee S, Durrett R (2009) Contact processes on random graphs with power law degree distributions have critical value 0. Ann Probab 37:2332–2356

Cox N, Subbarao K (2000) Global epidemiology of influenza: past and present. Annu Rev Med 51:407–421

Diekmann O, Heesterbeek J, Metz J (1990) On the definition and the computation of the basic reproduction ratio $\mathscr{R}_0$ in models for infectious diseases in heterogeneous populations. J Math Biol 28:365–382

Eames K, Keeling M (2002) Modeling dynamic and network heterogeneities in the spread of sexually transmitted diseases. Proc Nat Acad Sci 99:13330–13335

Earn D, Dushoff J, Levin S (2002) Ecology and evolution of the flu. Trends Ecol Evol 17:334–340

El Rhaffouli H, Laraqui A, Bajjou T, Melloul M, Obeid S et al (2014) Evolution of the Hemagglutinin gene of the influenza A (H1N1) pdm09 virus in Morocco during two influenza seasons 2009–2011. Curr Microbiol 68(3):372–380

Feld S (1991) Why your friends have more friends than you do. Am J Sociol 96:1464–1477

Garten RJ, Davis CT, Russell CA, Shu B, Lindstrom S, Balish A et al (2009) Antigenic and genetic characteristics of swine-origin 2009 a (H1N1) influenza viruses circulating in humans. Science 325(5937):197–201

Hethcote H, Van Ark J (1987) Epidemiological models for heterogeneous populations: proportionate mixing, parameter estimation, and immunization programs. Math Biosci 84:85–118

Hoschler K, Thompson C, Andrews N, Galiano M, Pebody R, Ellis J, Stanford E, Baguelin M, Miller E, Zambon M (2012) Seroprevalence of influenza A (H1N1) pdm09 virus antibody, England, 2010 and 2011. Emerg Infect Dis 18(11):1894

House T, Keeling M (2010) Insights from unifying modern approximations to infections on networks. J R Soc Interface 8:67–73

Kang S, Yang IS, Lee JY, Park Y et al (2010) Epidemiologic study of human influenza virus infection in South Korea from 1999 to 2007: origin and evolution of A/Fujian/411/2002-like strains. J Clin Microbiol 48(6):2177–2185

Keeling MJ (1999) The effects of local spatial structure on epidemiological invasions. Proc R Soc B 266:859–867

Kermack W, McKendrick A (1927) A contribution to the mathematical theory of epidemics. Proc R Soc Lond Ser A 115:700–721

Kiss I, Miller J, Simon P (2017) Mathematics of epidemics on networks: from exact to approximate models, vol 46. Springer, Berlin

Klein E, Serohijos AWR, Choi J, Shakhnovich E, Pekosz A (2014) Influenza A H1N1 pandemic strain evolution–divergence and the potential for antigenic drift variants. PLoS ONE 9:1–10

Kucharski A, Lessler J, Read J, Zhu H et al (2015) Estimating the life course of influenza A(H3N2) antibody responses from cross-sectional data. PLoS Biol 13:1–16
Leventhal GE, Hill AL, Nowak MA, Bonhoeffer S (2015) Evolution and emergence of infectious diseases in theoretical and real-world networks. Nature Commun 6:6101
Lindquist J, Ma J, van den Driessche P, Willeboordse F (2011) Effective degree network disease models. J Math Biol 62:143–164
Miller J (2011) A note on a paper by Erik Volz: SIR dynamics in random networks. J Math Biol 62:349–358
Miller J, Kiss I (2014) Epidemic spread in networks: existing methods and current challenges. Math Model Nat Phenom 9:4–42
Mills C, Robins J, Lipsitch M (2004) Transmissibility of 1918 pandemic influenza. Nature 432:904–906
Newman M (2002) The spread of epidemic disease on networks. Phys Rev Lett 66:016128
Pastor-Satorras R, Vespignani A (2001) Epidemic dynamics and endemic states in complex networks. Phys Rev E 63:066117
Pease C (1987) An evolutionary epidemiological mechanism, with applications to type A influenza. Theor Popul Biol 31:422–452
Perez C, Ferres M, Labarca J (2010) Pandemic (H1N1) 2009 reinfection, Chile. Emerg Infect Dis 16:156–157
Pourbohloul B, Meyers L, Skowronski D, Krajden M, Patrick D, Brunham R (2005) Modeling control strategies of respiratory pathogens. Emerg Infect Dis 11:1249–1256
Russell CA, Jones TC, Barr IG, Cox NJ et al (2008) The global circulation of seasonal influenza A (H3N2) viruses. Science 320(5874):340–346
Russo ML, Pontoriero AV, Benedetti E, Czech A et al (2014) Antigenic and genomic characterization of human influenza A and B viruses circulating in Argentina after the introduction of influenza A (H1N1) pdm09. J Med Microbiol 63(12):1626–1637
Strelkowa N, Lässig M (2012) Clonal interference in the evolution of influenza. Genetics 192(2):671–682
Taylor T, Kiss I (2014) Interdependency and hierarchy of exact and approximate epidemic models on networks. J Math Biol 69:183–211
van den Driessche P, Watmough J (2002) Reproduction numbers and sub-threshold endemic equilibria for compartmental models of disease transmission. Math Biosci 180:29–48
Volz E (2008) SIR dynamics in random networks with heterogeneous connectivity. J Math Biol 56:293–310
World Health Organization (2016) Fact sheet 211: influenza. http://www.who.int/mediacentre/factsheets/fs211/en/. Accessed 12 Apr 2017